Journal Pre-proof

Fast detecting hypochlorous acid based on electron-withdrawing group promoted oxidation and its biological applications in cells and root tips of plants

Ming Li, Jianbin Chao, Yaoming Liu, Miao Xu, Yongbin Zhang, Fangjun Huo, Juanjuan Wang, Caixia Yin

PII: S1386-1425(19)31400-3

DOI: https://doi.org/10.1016/j.saa.2019.118001

Reference: SAA 118001

To appear in: *Spectrochimica Acta Part A: Molecular and Biomolecular Spectroscopy*

Received date: 9 September 2019

Revised date: 23 December 2019

Accepted date: 25 December 2019

Please cite this article as: M. Li, J. Chao, Y. Liu, et al., Fast detecting hypochlorous acid based on electron-withdrawing group promoted oxidation and its biological applications in cells and root tips of plants, *Spectrochimica Acta Part A: Molecular and Biomolecular Spectroscopy*(2018), https://doi.org/10.1016/j.saa.2019.118001

Fast detecting hypochlorous acid based on electron-withdrawing group promoted oxidation and its biological applications in cells and root tips of plants

Ming Li,[ab] Jianbin Chao,[a] Yaoming Liu,[a] Miao Xu, [ab] Yongbin Zhang,[d] Fangjun Huo,[d] Juanjuan Wang[a] and Caixia Yin[c*]

[a]Scientific Instrument Center, Shanxi University, Taiyuan 030006, China

[b]School of Chemistry and Chemical Engineering, Shanxi University, Taiyuan 030006, China

[c]Institute of Molecular Science, Shanxi University, Taiyuan, 030006, China

[d]Research Institute of Applied Chemistry, Shanxi University, Taiyuan, 030006, China

*Corresponding author: C.X. Yin, E-mail: yincx@sxu.edu.cn,

Tel/Fax: +86-351-7011022.

Abstract: Hypochlorous acid, a type of reactive oxygen species, has been shown to play an important role in organisms. Nowadays, there are many kinds of fluorescence detecting mechanisms to detect hypochlorous acid in *vivo*. Due to the high selectivity, the mechanism of using the strong oxidation of hypochlorous acid to break carbon-carbon double bonds has been favored by many scientists. However, the reported probes of breaking carbon-carbon double bonds still had drawback such as slow response. Based on this, we introduced electron-withdrawing group malonitrile to accelerate the oxidation of hypochlorous acid, resulting in reaction time less than 150 s. Meanwhile, the probe exhibited excellent selectivity, optical stability, high sensitivity and the detection limit as low as 0.19 μM. More importantly, we also successfully proved the potential application of the probe for the detection of intracellular ClO^- living cells and Arabidopsis root tip by fluorescence imaging.

Key words: Electron-withdrawing group, Fluorescent probe, ClO^-, Imaging

1. Introduction

Hypochlorous acid (HClO)/Hypochlorite (ClO^-), as an important reactive oxygen species (ROS), is widely used in daily life and industry, such as drinking water disinfection, household bleach, cyanide treatment and cooling water treatment of coastal power stations [1-3]. At the same time, more and more scientific experiments have proved that moderate amount of HClO/ClO^- has a certain protective effect on human health [4-5], but the abnormal concentration of HClO in the body's cells will cause tissue destruction and cell damage [6-8]. Based on this, it is particularly important to study the physiological process of hypochlorous acid in the body [9].

Compared to traditional techniques, chemical probes based on absorption or fluorescence changes are more feasible for detecting analytes owing to their many appealing advantages such as low detection limit, high selectivity, real-time monitoring and its potential for in vivo imaging of living cells [10-11]. Therefore, it is a wise choice to use fluorescence probe strategy to detect HClO/ClO in vivo. At present, the detection of HClO/ClO^- by fluorescent probes is mainly based on the following mechanisms: oxidation of p-methoxyphenol to benzoquinone [12], oxime isomerization [13], chlorination of thioester and amide oxidation of p-aminophenol analogs [14,15], oxidation of thioethers into sulfonates [16,17], and cleavage of carbon-carbon double bonds [18]. Compared with among detection mechanisms, the mechanism of cleavage of carbon-carbon double bonds shows better selectivity and can effectively avoid interference of other reactive oxygen species [19]. However, the

cleavage of carbon-carbon double bonds generally requires a long reaction time, so it is a challenge to design a hypochlorous acid fluorescence probe with fast response speed and high selectivity.

Based on the above situation, we reasonably designed a probe **1** (2-((2E) - 1-(7-(diethylamino) - 2-oxo-2H-chromen-3-yl) - 3-(9-ethyl-9H-carbazol-3-yl) allylidene) malononitrile) to be used to detect ClO^-. In our design strategy, malononitrile is not only a linker between the coumarin and carbazole, but also can accelerate the oxidation of ClO^- as an electron-withdrawing group. After a series of spectral tests, the response time of the probe with $HClO/ClO^-$ was less than 150 s. Besides, the probe **1** had the advantages of good stability, low detection limit, high selectivity and sensitivity for the detection of hypochlorite. Furthermore, probe **1** also applied to monitor the fluctuation of ClO^- in HepG2 cells and Arabidopsis root tip successfully.

2. Materials and methods

2.1. Materials and measurement

All chemicals and reagents were purchased from Aladdin Reagent Shanghai Co., Ltd., all of which were of analytical grade. Distilled water was used throughout all experiments. ^1H NMR and ^{13}C NMR spectra were performed with Bruker instrument with TMS (Tetramethylsilane) as the internal standard for 600 MHz and 150 MHz spectrometer (AVAVCE Ⅲ HD), respectively. Shimadzu UV-2450 spectrophotometer and F-7000 fluorescence spectrophotometer (Hitachi, Japan) was employed to

measure absorption spectra and fluorescence spectra, respectively. Mass spectra were obtained with a Thermo Scientific Q Exactive LC-MS/MS system. The fluorescence images of probe were obtained using a ZEISS LSM 880 confocal laser scanning microscope.

2.2. Synthesis of compound 1

A mixture of 3-acetyl-7-diethylaminocoumarin (2.60 g, 10 mmol), malononitrile (1.25 mL, 20 mmol), acetic acid solution (0.45 mL, 8 mmol) and ammonium acetate (0.16 g, 2 mmol) was dissolved in 20 mL of benzene and heated to reflux with the aid of a water separator for 18h. After completion of the reaction, the solvent was evaporated, and a yellow oily substance was precipitated by adding 5 ml of ethanol, and then filtered under vacuum to give a crude product. Finally, the crude product was recrystallized from ethanol to give a yellow needle product (compound 1) (2.61g, yield 85 %). ^{1}H NMR (600 MHz, $CDCl_3$): δ 7.91 (s, 1H), 7.38 (d, *J* = 9.0 Hz, 1H), 6.66 (d, *J* = 8.9 Hz, 1H), 6.51 (s, 1H), 3.49 (q, *J* = 7.0 Hz, 4H), 2.69 (d, *J* = 12.8 Hz, 3H), 1.27 (t, *J* = 7.1 Hz, 6H).

*2.3 Synthesis of probe **1***

Compound 1 (0.307 g, 1 mmol), N-ethylcarbazole-3-carbaldehyde (0.223 g, 1 mmol) and 2 mL DES (deep eutectic solvent) were added into 10 mL round bottom flasks in turn and stirred for 1-2 hours at 30-40℃. The reaction was followed by TLC. After completion of the reaction, the mixture was cooled to room temperature, washed with distilled water, and the precipitate was filtered and dried to give an orange solid

(0.38 g， yield 75 %). ^{1}H NMR (600 MHz, DMSO-d_6): δ 8.64 (s, 1H), 8.20 (d, *J* = 7.6 Hz, 1H), 8.15 (s, 1H), 7.94 (d, *J* = 8.6 Hz, 1H), 7. 76–7.64 (m, 3H), 7.58 (d, *J* = 8.9 Hz, 1H), 7.52 (d, *J* = 13.9 Hz, 2H), 7.29–7.23 (m, 1H), 6.83 (d, *J* = 8.8 Hz, 1H), 6.69 (s, 1H), 4.49 (d, *J* = 7.3 Hz, 2H), 3.52 (d, *J* = 7.2 Hz, 4H), 1.33 (t, *J* = 6.8 Hz, 3H), 1.17 (t, *J* = 6.3 Hz, 6H). ^{13}C NMR (151 MHz, DMSO-d_6): δ 167.4, 158.8, 157.7, 152.5, 151.1, 147.1, 142.2, 140.7, 131.3, 127.5, 127.1, 126.0, 124.1, 123.4, 122.7, 121.3, 120.5, 120.4, 114.9, 114.1, 112.7, 110.6, 110.3, 110.2, 107.8, 96.9, 78.7,60.2, 44.9, 37.8,21.2, 14.3, 12.8. HRMS: m/z calculated for $C_{33}H_{29}N_4O_2$ $[M+H]^+$: 513.22458, obtained: 513.22891. (Fig.S1, S2, S3)

2.4 Measurement procedure

0.001 g of probe **1** was accurately weighed and dissolved in 2 mL of DMSO solution to obtain a 1 mM stock solution. The absorption and fluorescence spectra experiments were measured in C_2H_5OH/PBS (v/v, 1/1, pH 7.4). In the fluorescence spectroscopy experiment, the selected excitation wavelengths were 420 nm and the slits were 5/2.5 nm respectively. All substances in the selective experiment were dissolved or diluted with distilled water to make a stock solution of 0.1 M. CN^-, SCN^-, Br^-, MnO_4^- were obtained by dissolving its potassium salt. The remaining ions were obtained by dissolving the sodium salt.

2.5 Cell culture and fluorescence imaging

HepG2 cells were cultured in Dulbecco's Modified Eagle Medium (DMEM) supplemented with 12 % (v/v) fetal bovine serum (FBS) and 1 % antibiotics at 37 ℃

in a 5 % CO_2 incubator, and replaced culture media with fresh media every day. The cells were plated into 6 well culture-plates and incubated for 24 h to allow the cells adhere. The fluorescence images of probe were obtained using a ZEISS LSM 880 confocal laser scanning microscope. And fluorescence imaging at blue channel (410-500nm), the excitation wavelength was 405 nm.

2.6 Arabidopsis thaliana culture and fluorescence imaging

The culture of Arabidopsis thaliana was cultured according to the methods in the literature [20]. The root tip of Arabidopsis thaliana was selected as the experimental object. The fluorescence images of probe were obtained using a ZEISS LSM 880 confocal laser scanning microscope. And fluorescence imaging at blue channel (410-500nm), the excitation wavelength was 405 nm.

3. Results and discussion

*3.1 Time response and optical stability study of probe **1***

Before spectral titration, we first determined the stability of **1** and the reaction time with ClO^- by time-dependent study in C_2H_5OH/PBS (v/v, 1/1, pH 7.4). Fig. 1 displayed the change in fluorescence intensity at 490 nm of the **1** with an excitation 420 nm in 10 minutes. The probe **1** also exhibited good stability. When ClO^- was added, the fluorescence intensity reached a maximum around 3 minutes and remained stable.

Insert Fig.1

*3.2 Spectroscopic characteristics of probe **1***

The spectroscopic experiment of **1** (10 μM) for detecting ClO^- was carried out in C_2H_5OH/PBS (v/v, 1/1, pH 7.4). As shown in Fig. 2a, **1** itself had a weak absorption peak at 410 nm. With the addition of ClO^-, the absorption at 475 nm gradually decreased up to disappear, and new absorption appeared at 410 nm, at the same time the color of the solution changed from orange to colorless. Subsequently, we found that **1** exhibited a good linear relationship with ClO^- in the concentration range of 147.4-522.6 μM. The regression equation was A=0.271×[ClO^-]-4.448，R^2=0.99626 (Fig. 2b).

Inset Fig.2

The changes in the fluorescence spectra of **1** (10 μM) in C_2H_5OH/PBS (v/v, 1/1, pH 7.4) system were shown in Fig. 3a. As we can see, with the addition of ClO^- (0 – 469 μM), **1** produced a distinct fluorescent signal at 490 nm. It is speculated that the changes in the ultraviolet and fluorescence spectra resulting from the strong oxidative nature of ClO^- cleaving double bond to form a new compound, N-ethylcarbazole-3-carbaldehyde. Therefore, we dissolved the molecular in DMSO and performed fluorescence detection in the test system. The emission wavelength of the molecular is almost same as the emission wavelength of the **1** (Fig. S4). The fluorescence intensity enhanced linearly with the ClO^- concentration from 93.8-361.8 μM. The linear equation could be represented by F=11.972×[ClO^-]-1100.071 with the correlation coefficient of R^2 = 0.9942 (Fig.3b). The detection limit was calculated to be 0.19 μM according to the IUPAC standard method LOD=3δ/k. These data

demonstrated that **1** could achieve quantitative detection of ClO^-.

Inset Fig.3

*3.3 The selective response of probe **1***

Excellent selectivity and anti-interference performance are key parameters for evaluating the suitability of a probe for biological applications. Therefore, we evaluated the selectivity of **1** for ClO^- by adding an excess of different anions, strong oxidizing substances or some common nucleophilic thiols. As could be seen in Fig. 4, the addition of other analytes each did not cause significant fluorescence changes in the probe **1** system. We further added different analytes to **1**, and then added 469 μM ClO^- to detect the anti-interference ability of **1**. Those results showed that **1** has excellent selectivity and anti-interference ability for ClO^- detection.

Inset Fig.4

*3.4 The effect of pH for probe **1***

Next, we tested the fluorescence response of **1** to ClO^- in different pH environments (pH 3-9). As observed in Fig. 5, **1** had no significant difference in fluorescence intensity between pH 3-9. When 469 μM ClO^- was added, **1** showed the largest response signal to ClO^- only in the pH 7.4 environment. Therefore, **1** could be used to monitor ClO^- without being affected by physiological pH.

Inset Fig.5

3.5 Proposed mechanism

We further explored the recognition mechanism of probe **1** for ClO^- by NMR

titration. The olefin in the **1** structure was easily oxidized by ClO^- to an epoxy compound and then formed an aldehyde (Scheme 2). As Fig. S5 shown, after the addition of ClO^-, a new peak appeared at a chemical shift of 10.04 ppm, which was attributed to the aldehyde group peak. The other peaks shifted to higher field. The suggested mechanism cleavage is accordance with the absorption and fluorescence spectra.

Inset Scheme 2

3.6 Cellular imaging

Based on the excellent characteristics of the above probe **1** in vitro, we applied **1** to HepG2 intracellular imaging to detect exogenous ClO^-. HepG2 cells were incubated with **1** (5 μM) for 15 min and then washed three times with PBS buffer. Fig. 6 A1 and A2 showed that there is almost no fluorescence change in the cells under the blue channel. However, after treated with 154.1 μM ClO^- for 30 min and then washed three times with PBS buffer in which an obvious fluorescence signal was appeared in blue channel (B1 and B2). All the results illustrated that **1** could be used to monitor ClO^- in living cells.

Inset Fig.6

3.7 Arabidopsis thaliana imaging

In order to verify that the probe **1** has better cell permeability, we also performed Arabidopsis root tip imaging. Arabidopsis root tips were firstly incubated with **1** for 30 min and washed three times. After co-incubation of **1** and Arabidopsis root tips,

incubation with ClO^- continuously for 40 min. As shown in Fig.7, there was a significant fluorescence change from A1 to B1 under blue channel. This was consistent with the phenomenon of fluorescence imaging in cells. Those data showed that **1** had good cell permeability and could be successfully applied to the root tip of plants.

Inset Fig.7

4. Conclusions

In summary, we designed and synthesized a fluorescent probe **1** with electron-withdrawing group as an accelerator for the detection of ClO^-. The addition of ClO^- caused **1** to produce a strong fluorescence emission at a wavelength of 490 nm and exhibited a good linear relationship in the concentration range of 147.4-522.6 μM. **1** showed excellent time response to ClO^- less than 150s. Simultaneously, the probe exhibited good selectivity, optical stability, high sensitivity and low detection. Furthermore, the results of fluorescence imaging confirmed that **1** can be applied to HepG2 cells and Arabidopsis root tip to identify exogenous ClO^-. Most importantly, it will provide a new idea to improve the reaction speed between the probe and HClO to realize in *situ* detection of HClO in *vivo*.

Acknowledgements

This work was supported by the National Natural Science Foundation of China (No. 21775096, 21672131), Natural Science Foundation of Shanxi Province of China (No.

201701D121018), One hundred people plan of Shanxi Province, Shanxi Province "1331 project" key innovation team construction plan cultivation team (2018-CT-1), Shanxi Province Foundation for Returness (2017-026), Shanxi Collaborative Innovation Center of High Value-added Utilization of Coal-related Wastes, 2018 xiangyuan county solid waste comprehensive utilization Science and technology project (2018XYSDJS-05), the Shanxi Province Science Foundation for Youths (No. 201901D111015), Key R&D Program of Shanxi Province (201903D421069), and Scientific Instrument Center of Shanxi University (201512).

References

[1] L.D. Chen, H.L. Ding, N. Wang, Y. An, C.W. Lü, Two highly selective and sensitive fluorescent probes design and apply to specific detection of hypochlorite，Dyes. Pigments 161 (2019) 510-518.

[2] W.Y. Lin, L.L. Long, B.B. Chen, W. Tan, A ratiometric fluorescent probe for hypochlorite based on a deoximation reaction, Chemistry 15 (2009) 2305-2309.

[3] K. Vijayaraghavan, T.K. Ramanujam, N. Balasubramanian, In situ hypochlorous acid generation for the treatment of textile wastewater, Color. Technol. 117 (2006) 49-53.

[4] A.L. Chapman, R. Senthilmohan, C.C. Winterbourn, A.J. Kettle, Arch，Comparison of mono- and dichlorinated tyrosines with carbonyls for detection of hypochlorous acid modified proteins, Biochem. Biophys. 377 (2000) 95-100.

[5] Y. Zhou, J.Y. Li, K.H. Chu, K. Liu, C. Yao, J.Y. Li, Fluorescence turn-on detection of hypochlorous acid via HOCl-promoted dihydrofluorescein-ether oxidation and its application in vivo, Chem. Commun. 48 (2012) 4677-4679.

[6] J.W. Li, C.X. Yin, T. Liu, Y. Wen, F.J. Huo, A new mechanism-based fluorescent probe for the detection of ClO- by UV–vis and fluorescent spectra and its applications, Sens. Actuat. B-Chem. 252 (2017) 1112-1117.

[7] H.H. Song, Y.M. Zhou, C.G. Xu, X. Wang, J.L. Zhang, Y. Wang, X.Q. Liu, M.X. Guo, X.J. Peng, A dual-function fluorescent probe: Sensitive detection of water content in commercial products and rapid detection of hypochlorite with a large

Stokes shift, Dyes. Pigments 162 (2018) 160-167.

[8] X. Han, C. Tian, J. Jiang, M.S. Yuan, S.W. Chen, J. Xu, T. Li, J. Wang, Two Ratiometric Fluorescent probes for hypochlorous acid detection and imaging in living cells, Talanta 186 (2018) 65-72.

[9] Y.K. Yue, F.J. Huo, C.X. Yin, J.O. Escobedo, R.M. Strongin, Recent progress in chromogenic and fluorogenic chemosensors for hypochlorous acid, Analyst 141 (2016) 1859-1873.

[10] M.G. Ren, Z. Kai, L.W. He, W.Y. Lin, Mitochondria and lysosome-targetable fluorescent probes for HOCl: recent advances and perspectives, J. Mater. Chem. B (2018) 1716.

[11] X. Wang, Y. Zhou, C. Xu, H. Song, L. Li, J. Zhang, M. Guo, A highly selective fluorescent probe for the detection of hypochlorous acid in tap water and living cells, Spectrochim. Acta A 203 (2018) 415-420.

[12] W.J. Zhang, C. Guo, L.H. Liu, J.G. Qin, C.L. Yang, Naked-eye visible and fluorometric dual-signaling chemodosimeter for hypochlorous acid based on water-soluble p-methoxyphenol derivative, Org. Biomol. Chem. 9 (2011) 5560-5563.

[13] S.Y. Yu, C.Y. Hsu, W.C. Chen, L.F. Wei, S.P. Wu, A hypochlorous acid turn-on fluorescent probe based on HOCl-promoted oxime oxidation and its application in cell imaging, Sens. Actuat. B-Chem. 196 (2014) 203-207.

[14] X.H. Zhou, Y.R. Jiang, X.J. Zhao, D. Guo, A naphthalene-based two-photon fluorescent probe for selective and sensitive detection of endogenous hypochlorous

acid, Talanta 160 (2016) 470-474.

[15] W.Z. Yin, H.J. Zhu, R.Y. Wang, A sensitive and selective fluorescence probe based fluorescein for detection of hypochlorous acid and its application for biological imaging, Dyes. Pigments 107 (2014) 127-132.

[16] J.Y. Hwang, M.J. Choi, J. Bae, S.K. Chang, Signaling of hypochlorous acid by selective deprotection of dithiane, Org. Biomol. Chem. 9 (2011) 7011.

[17] S. Kenmoku, Y. Urano, H. Kojima, T. Nagano, Development of a highly specific rhodamine-based fluorescence probe for hypochlorous acid and its application to real-time imaging of phagocytosis, J. Am. Chem. Soc. 129 (2007) 7313-7318.

[18] J.F. Li, P.F. Li, F.J. Huo, C.X. Yin, T. Liu, J.B. Chao, Y.B. Zhang, Ratiometric fluorescent probes for ClO − and invivo applications, Dyes. Pigments 130 (2016) 209-215.

[19] L. Zhou, D.Q. Lu, Q. Wang, S. Hu, H. Wang, H. Sun, X. Zhang, A high-resolution mitochondria-targeting ratiometric fluorescent probe for detection of the endogenous hypochlorous acid, Spectrochim. Acta A 166 (2016) 129-134.

[20] E. Syslová, P. Landa, L.R. Stuchlíková, P. Matoušková, L. Skálová, B. Szotáková, M. Navrátilová, T. Vaněk, R. Podlipná, Metabolism of the anthelmintic drug fenbendazole in Arabidopsis thaliana and its effect on transcriptome and proteome, Chemosphere 218 (2019) 662-669.

Figure captions

Scheme 1. The synthetic route of probe **1**.

Scheme 2. Response mechanism of probe **1** to ClO^-.

Fig.1 Time-dependent fluorescence intensity of probe **1** before and after the addition of ClO^- in C_2H_5OH/PBS (v/v, 1/1, pH 7.4). λ_{ex} = 420 nm, slit: 5nm/2.5nm.

Fig.2 (a) The absorption spectra of probe **1** (10 μM) vary with increasing ClO^- (469 μM) concentration in C_2H_5OH/PBS (v/v, 1/1, pH 7.4); inset: the color changes from orange to colorless. (b) Linear fit between absorbance (475 nm) and ClO^- concentration (147.4-522.6 μM); inset: the absorbance of probe 1 at 475 nm.

Fig.3 (a) The fluorescence spectrum of probe **1** (10 μM) in the presence of different concentration of ClO^- (0-469 μM) in C_2H_5OH/PBS (v/v, 1/1, pH 7.4). (b) Linear fit between the fluorescence intensity (490 nm) and ClO^- concentration (93.8-361.8 μM). λ_{ex}=420nm, slit: 5 nm/2.5 nm.

Fig.4 Fluorescence intensity of probe **1** (10 μM) towards ClO^- in C_2H_5OH/PBS (v/v, 1/1, pH 7.4) in the absence and presence of 200 μM various analytes (F^-, Cl^-, Br^-, HCO_3^-, SO_4^{2-}, SO_3^{2-}, S^{2-}, CO_3^{2-}, CNS^-, AC^-, NO_3^-, HSO_3^-, CN^-, Cys, GSH, Hcy, H_2O_2, MnO_4^{2-}). λ_{ex}=420nm, slit: 5 nm/2.5 nm.

Fig.5 Fluorescence intensity of the probe **1** (10 μM) at different pH values in the absence or presence of ClO^- (469 μM) in C_2H_5OH/PBS (v/v, 1/1, pH 7.4). λ_{ex}=420nm, slit: 5 nm/2.5 nm.

Fig.6 (A1-A2) Confocal fluorescence images of HepG2 cells incubated with probe **1**

(5 μM) for 15 min (A1, blue channel); (B1-B2) Confocal fluorescence images of HepG2 cells were further cultured with ClO^- (154.1 μM) for 10 min (B1, blue channel). Fluorescence images of HepG2 cells were indicated by blue channel (λ_{ex} = 405nm, λ_{em} = 410-500 nm).

Fig.7 (A1-A2) Confocal fluorescence images of Arabidopsis root tip with probe **1** (10 μM) for 30 min (A1, blue channel); (B1-B2) Confocal fluorescence images of co-incubation of **1** and Arabidopsis root tips towards addition of ClO^- (154.1 μM) for 40 min (B1, blue channel). Blue channel: λ_{ex} = 405nm, λ_{em} = 410-500 nm.

Figures

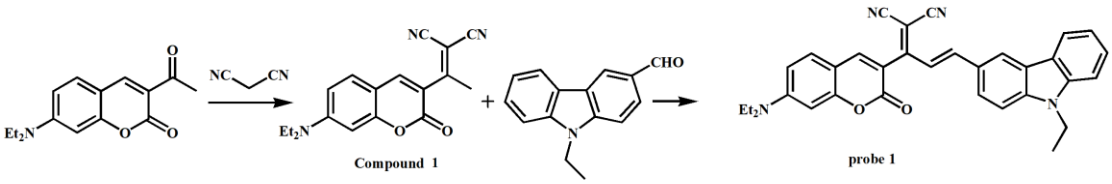

Scheme 1. The synthetic route of probe **1**.

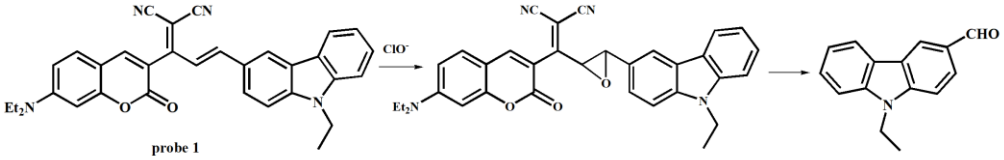

Scheme 2. Response mechanism of probe **1** to ClO^-.

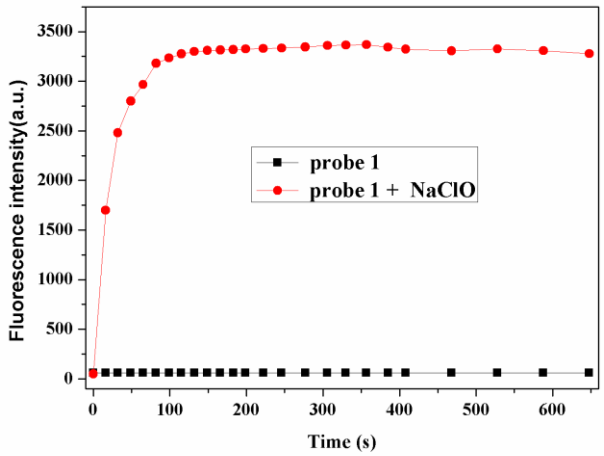

Fig.1 Time-dependent fluorescence intensity of probe **1** before and after the addition of ClO^- in C_2H_5OH/PBS (v/v, 1/1, pH 7.4). λ_{ex} = 420 nm, slit: 5nm/2.5nm.

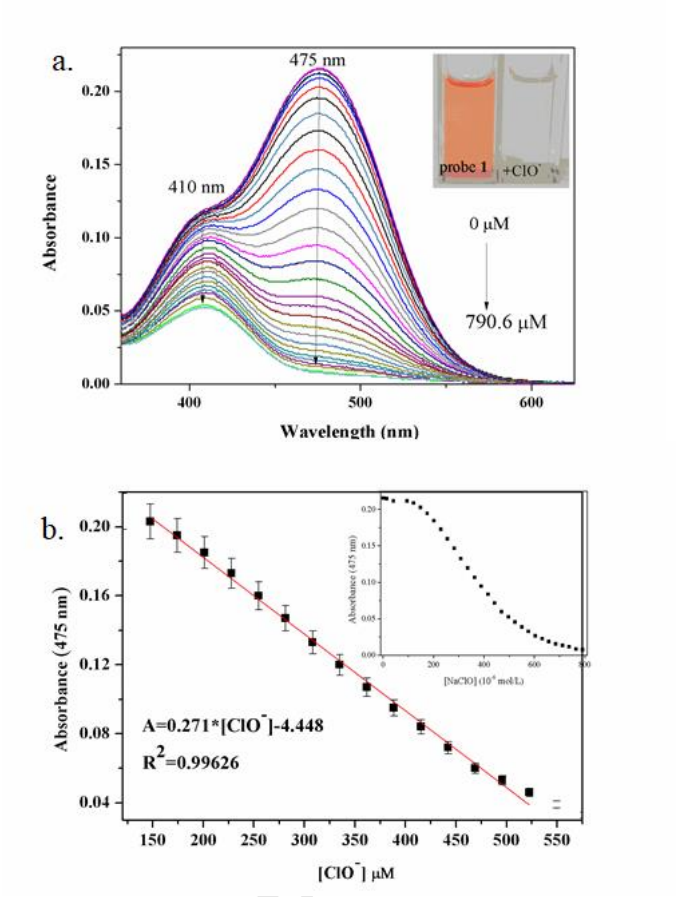

Fig.2 (a) The absorption spectrum probe **1** (10 μM) vary with increasing ClO^- (469 μM) concentration in C_2H_5OH/PBS (v/v, 1/1, pH 7.4); inset: the color changes from orange to colorless. (b) Linear fit between absorbance (475nm) and ClO^- concentration (147.4-522.6 μM); inset: the absorbance of probe **1** at 475 nm.

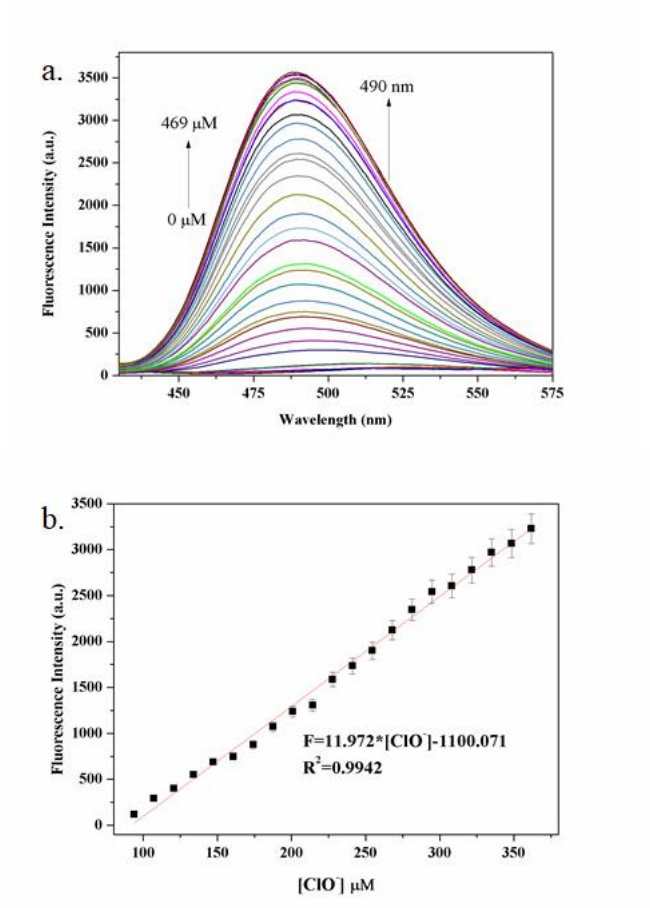

Fig.3 (a) The fluorescence spectrum of probe **1** (10 μM) in the presence of different concentration of ClO^- (0-469 μM) in C_2H_5OH/PBS (v/v, 1/1, pH 7.4). (b) Linear fit between the fluorescence intensity (490 nm) and ClO^- concentration (93.8-361.8 μM). λ_{ex}=420nm, slit: 5 nm/2.5 nm.

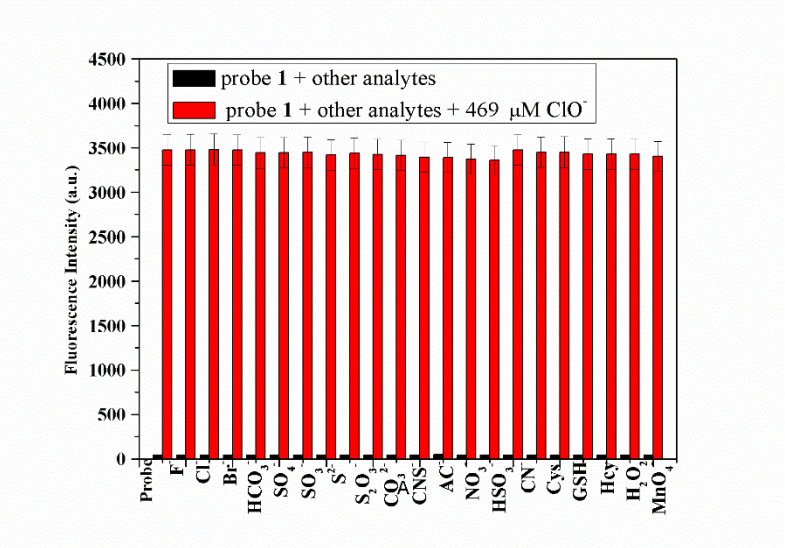

Fig.4 Fluorescence intensity of probe **1** (10 μM) towards ClO^- in C_2H_5OH/PBS (v/v, 1/1, pH 7.4) in the absence and presence of 200 μM various analytes (F^-, Cl^-, Br^-, HCO_3^-, SO_4^{2-}, SO_3^{2-}, S^{2-}, CO_3^{2-}, CNS^-, AC^-, NO_3^-, HSO_3^-, CN^-, Cys, GSH, Hcy, H_2O_2, MnO_4^{2-}). λ_{ex}=420nm, slit: 5 nm/2.5 nm.

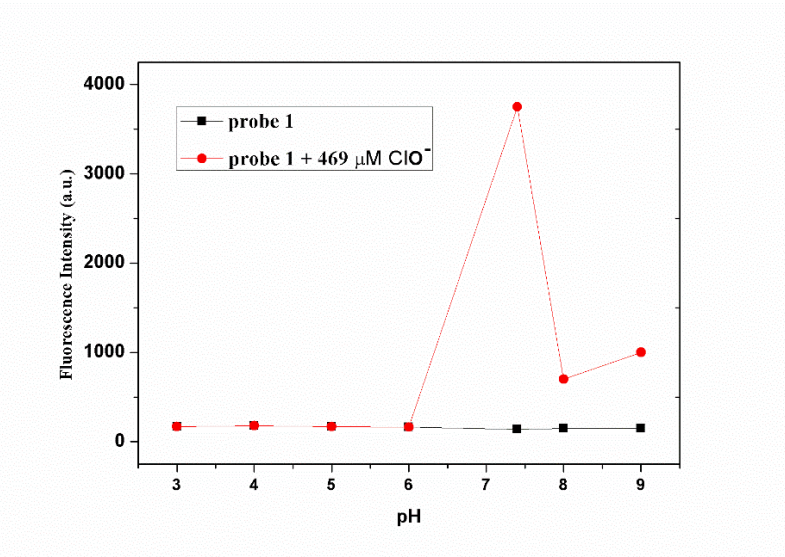

Fig.5 Fluorescence intensity of the probe **1** (10 μM) at different pH values in the absence or presence of ClO^- (469 μM) in C_2H_5OH/PBS (v/v, 1/1, pH 7.4). λ_{ex}=420nm, slit: 5 nm/2.5 nm.

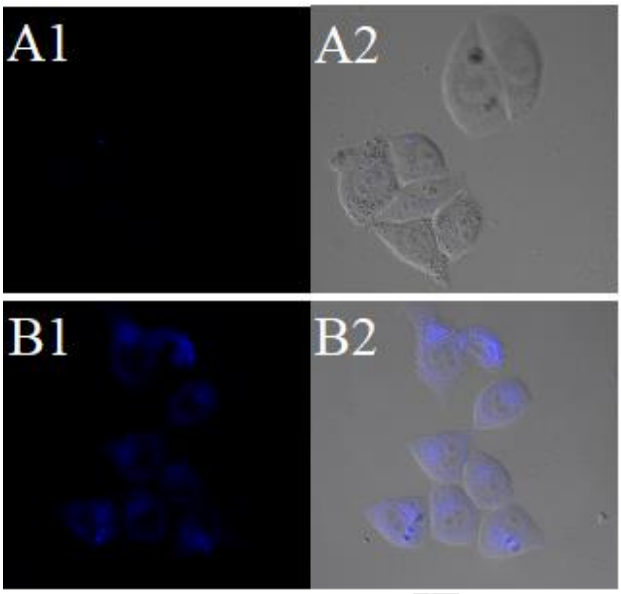

Fig.6 (A1-A2) Confocal fluorescence images of HepG2 cells incubated with probe **1** (5 μM) for 15 min (A1, blue channel); (B1-B2) Confocal fluorescence images of HepG2 cells were further cultured with ClO^- (154.1 μM) for 10 min (B1, blue channel). Fluorescence images of HepG2 cells were indicated by blue channel (λ_{ex} = 405nm, λ_{em} = 410-500 nm).

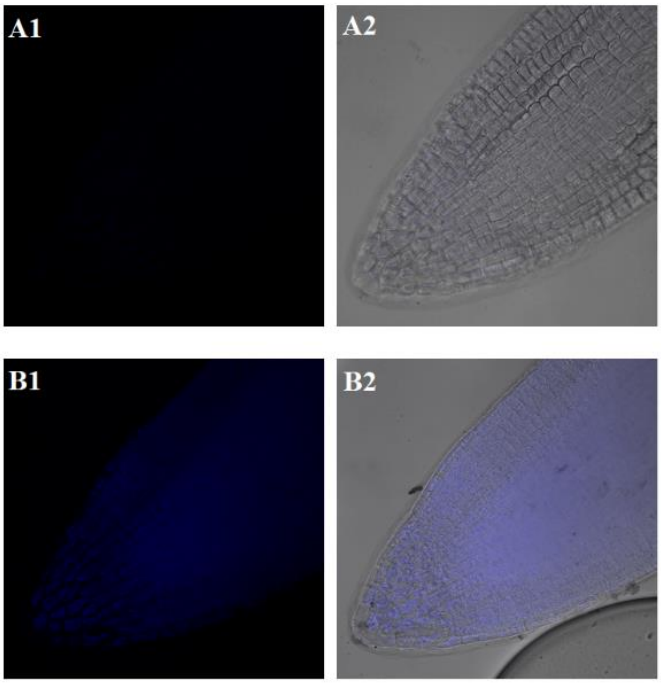

Fig.7 (A1-A2) Confocal fluorescence images of Arabidopsis root tip with probe **1** (10 μM) for 30 min (A1, blue channel); (B1-B2) Confocal fluorescence images of co-incubation of **1** and Arabidopsis root tips towards addition of ClO^- (154.1 μM) for 40 min (B1, blue channel). Blue channel: λ_{ex} = 405nm, λ_{em} = 410-500 nm.

Author contributions

Ming Li and Miao Xu carried out synthesis and spectrometry
Juanjuan Wang's cell imaging
Caixia yin and Fangjun huo's idea and writing
Jianbin Chao and Yaoming Liu's NMR
Yongbin Zhang's sample detection.

Declaration of interest statement

We have no any interest conflict.

Graphic

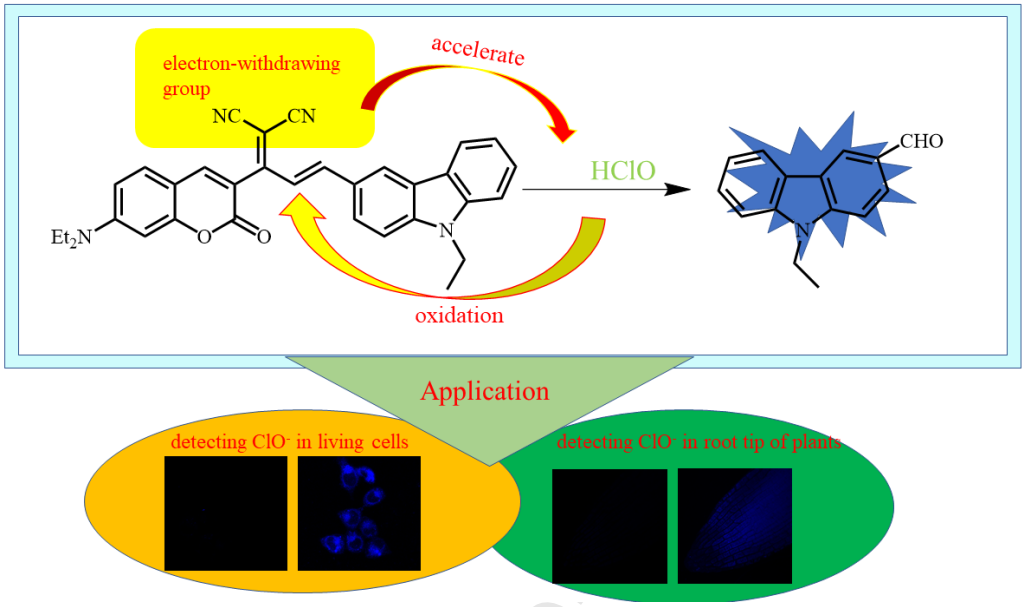

Highlights

1. A novel fluorescent probe with electron-withdrawing group as an accelerator for the detection of ClO^-.
2. The probe exhibited good selectivity, optical stability, high sensitivity and low detection.
3. The probe can be applied to HepG2 cells and Arabidopsis root tip to identify exogenous ClO^-.